Friction **2**(2): 106–113 (2014)
DOI 10.1007/s40544-014-0052-4
ISSN 2223-7690
CN 10-1237/TH
REVIEW ARTICLE

Superlubricity on the nanometer scale

Ernst MEYER[1,*], **Enrico GNECCO**[2]

[1] *Department of Physics, University of Basel, Klingelbergstr. 82, 4056 Basel, Switzerland*

[2] *IMDEA Nanociencia, Campus Universitario de Cantoblanco, Calle Faraday 9, 28049 Madrid, Spain*

Received: 31 March 2014 / Revised: 28 April 2014 / Accepted: 14 May 2014

Abstract: The transition from atomic stick-slip to continuous sliding has been observed in a number of ways. If extended contacts are moved in different directions, so-called structural lubricity is observed when the two surface lattices are non-matching. Alternatively, a "superlubric" state of motion can be achieved if the normal force is reduced below a certain threshold, the temperature is increased, or the contact is actuated mechanically. These processes have been partially demonstrated using atomic force microscopy, and they can be theoretically understood by proper modifications of the Prandtl–Tomlinson model.

Keywords: structural lubricity; dynamic superlubricity; atomic force microscopy; friction force microscopy; themolubricity; Prandtl–Tomlinson model

1 Introduction

Controlling light sources or home appliances by electrical switches is everyday's experience. However, we are not used to control friction in an analogous way. Recent friction experiments on the nanometer scale have shown that the transition from a high friction state to a low friction state is possible by changing some easily accessible parameters, such as the reciprocal orientation of contacts or the application of electrostatic forces. Therefore, we might have the possibility to switch friction on and off in the near future, at least on the nanometer scale.

2 Structural superlubricity

If two crystal surfaces are non-matching, a reduction of friction is expected when the surfaces slide past each other. In the one-dimensional case, the Frenkel–Kontorova (FK) model [1] predicts that an infinite molecular chain, incommensurable with the substrate, would experience zero friction. The same is expected for the two-dimensional contact between two non-matching surface lattices. A robust confirmation of these predictions came from the experiments performed in the groups of Israelachvili and Hirano using the surface force apparatus [2, 3], i.e., an instrument in which the forces between two curved molecularly smooth mica surfaces pressed into contact can be accurately measured by optical interferometry.

Hirano et al. also observed what they called `superlubricity' in scanning tunneling microscope (STM) measurements with a monocrystalline tungsten tip sliding on a Si(001) surface. However, questionable analogies to superconductivity and superfluidity may arise, and the term `structural lubricity', introduced by Müser [4] is also used to define the experimental situation in which a state of ultralow friction is achieved when the contacting surfaces are incommensurate. The most convincing demonstration of this effect so far came probably from the measurements by Dienwiebel et al. [5], who moved a small graphite flake with different orientations with respect to a graphite surface using a dedicated atomic force microscopy (AFM) setup. As shown in Fig. 1, an increase of friction is observed when the main crystallographic directions of flake and substrate coincide

* Corresponding author: Ernst MEYER.
E-mail: ernst.meyer@unibas.ch

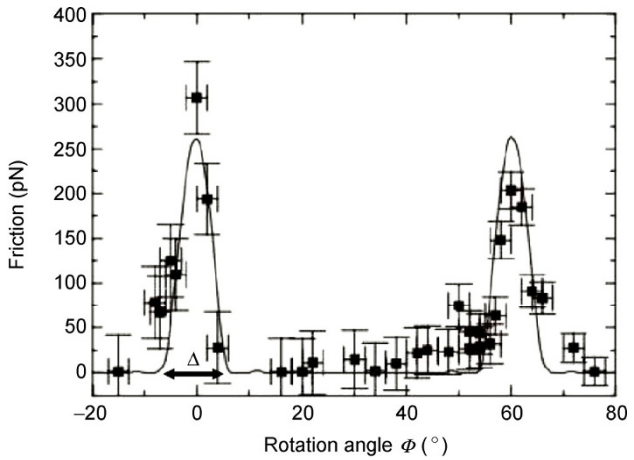

Fig. 1 Friction of graphite flake vs. orientation relative to the graphite surface. For 0 and 60° an increase is observed. Inbetween friction is reduced because of the incommensurability of the contacts [5].

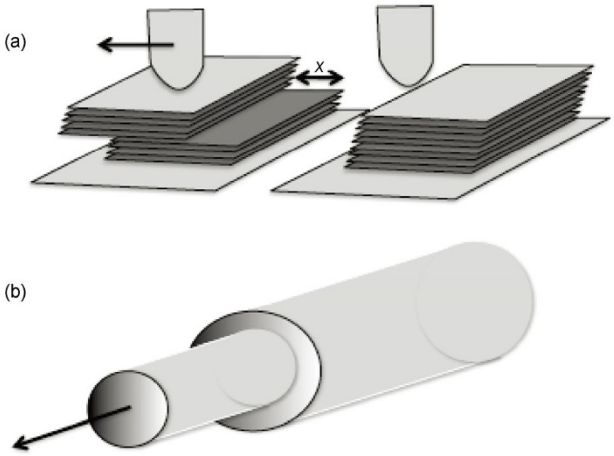

Fig. 2 (a) Displacement and self-retracting motion of a graphite microflake. The motion has been observed by an electron microscope or other optical setups. (b) Schematic diagram of the telescopic extension of a multiwalled carbon nanotube.

(at 0 or 60°), whereas the friction is reduced for intermediate angles. This corresponds well to the expectation that a commensurate contact with interlocking atoms gives maximum friction, whereas an incommensurate character of the contact leads to a reduction of friction. Note that the width of the friction peaks, Δ, is theoretically related to the diameter of the flake, D, by the formula $\tan\Delta = a/D$, where a is the unit cell length [6]. A comparison with the measurements by Dienwiebel et al. suggests that the graphite flake had a diameter of few nanometers.

More recent investigations have focused on the stability of incommensurate sliding contacts [7]. The mechanical torque appearing in such case was found to result in sudden rotations, which limits the lifetime of the superlubric state. Numeric simulations also suggested that the superlubric state is preserved in large flakes sliding at low temperatures and high velocities (some m/s) [8]. An experimental realization is shown in Fig. 2(a), which shows how the flakes of graphite are displaced by the action of a probing tip as suggested by electron microscopy observations [7–9]. When the tip releases the upper layers of the flake, these layers self-retract to the original position, also called self-retracting motion (SRM). With the help of an optical setup, the motion of the microflake was time-resolved. The observed maximum speeds of 25 m/s are already close to the theoretical maximum speed, v_{max}, reached under the assumption of negligible friction and constant acceleration across the distance x compared to the full width L,

$$v_{\max} = 2\sqrt{\frac{x}{L}\frac{\gamma}{m}},$$

where γ is the surface energy gained by self-retraction and m is the mass of the microflake. Therefore, superlubricity seems to be retained up to these high speeds. However, SRM also shows cases of sliding at a constant velocity, which depends on temperature and is most probably related to some defects. A logarithmic increase of the saturation velocity with temperature indicates thermal activation effects with activation energies of the order of 0.1 to 0.7 eV, possibly related to defects at the boundary of the flakes.

Other experimental observations of structural superlubricity have been also reported on MoS_2 [10] and Ti_3SiC_2 [11]. Indications of superlubricity were also observed in the telescopic extension and retraction of multiwalled carbon nanotubes, which showed no signs of wear after many repetitions [12, 13]. These telescopic extensions and retractions can also be applied for high frequency mechanical oscillators [14, 15].

Very recently, a remarkable observation of structural lubricity has been reported by Kawai et al., who pulled up polymer chains from a gold surface using AFM in a dynamic mode [16]. Kawai's experiment was performed in ultra-high vacuum at very low temperature (4K). Under those conditions, it was

possible to measure the force gradients accompanying the detachment of individual polymer chains with extremely high accuracy (Fig. 3). The primary observation is the modulation of the force during detachment of fluorene groups, which could be precisely related to the adhesion energy of these submolecular groups by a theoretical analysis based on an extended FK model and realistic interaction potentials. A small modulation of the force gradient due to the sliding on the gold surface was also observed, which demonstrates that the sliding of the polymer chain is in the superlubric state due to the incommensurability between the atomic spacing of the gold substrate and the equilibrium distance between consecutive fluorene units.

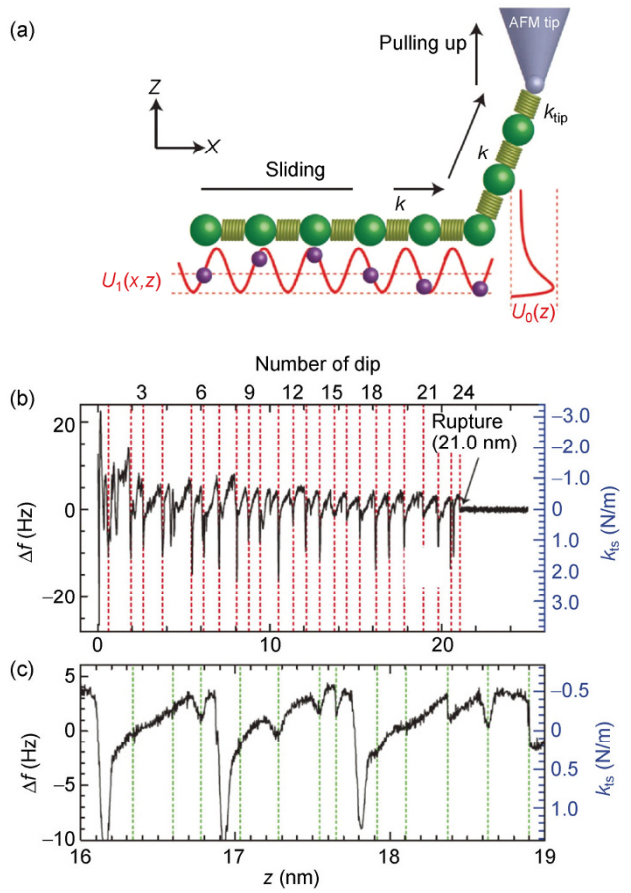

Fig. 3 (a) Sketch (side view) of a polymer chain consisting of fluorene initially lying on a Au(111) surface and pulled up by an AFM tip. (b) The force gradient variations show periodic variations due to the detachment of the fluorene units. (c) The zoom on the lower right shows a small variation due to the sliding of the molecular chain on the substrate, which demonstrates practically frictionless motion because of the incommensurability of the substrate periodicity and the molecular spacing. The measurements also demonstrated that the intramolecular stiffness is relatively large (around 200 N/m) which makes elastic deformation to accommodate the molecule on the substrate unfavourable [16].

3 Static and dynamic superlubricity

The most direct way to achieve superlubricity when a sharp nanotip is sliding on an atomically flat surface is reducing the normal force. According to the Prandtl–Tomlinson (PT) model the transition from atomic stick slip to smooth sliding occurs when a characteristic parameter η reaches the critical value $\eta_c = 1$. The parameter η is defined by the ratio of the amplitude of the periodic surface potential U_0 and the strain energy stored in the elastic support driving the nanotip [17]:

$$\eta = \frac{4\pi^2 U_0}{ka^2},$$

where k is an effective (lateral) stiffness of the system. Typical values in force microscopy experiments are $k = 1$ N/m and $a = 0.5$ nm, which would mean that for $E_0 < 0.08$ eV superlubricity is expected. Socoliuc et al. have observed this transition experimentally for an AFM tip sliding on a NaCl(001) surface in ultra-high vacuum (Fig. 4). When the normal force is below 1 nN the corresponding values of η cross the critical value and smooth sliding is observed. For larger forces a typical atomic-scale stick-slip is observed. In this case the probing tip periodically ends up in elastic instabilities, and suddenly slips, every time the lateral force gradient equals the spring constant k. From a technical point of view, it is interesting to observe that the values of k are in the order of N/m, which clearly shows that the effective stiffness is essentially determined by the contact region and not by the elastic support of the tip (i. e., a microfabricated cantilever, the lateral spring constant of which is typically two orders of magnitude larger than the measured values of k). It is also interesting to compare the dependence of the average lateral force <F> with the parameter η, as expected from the PT model (Fig. 5(a)), with the measurements on NaCl (Fig. 5(b)). The values of η can be indeed estimated from the friction loops, as detailed in Ref. [17], and in the experiment by Socoliuc et al., η turned out to be proportional to the normal force.

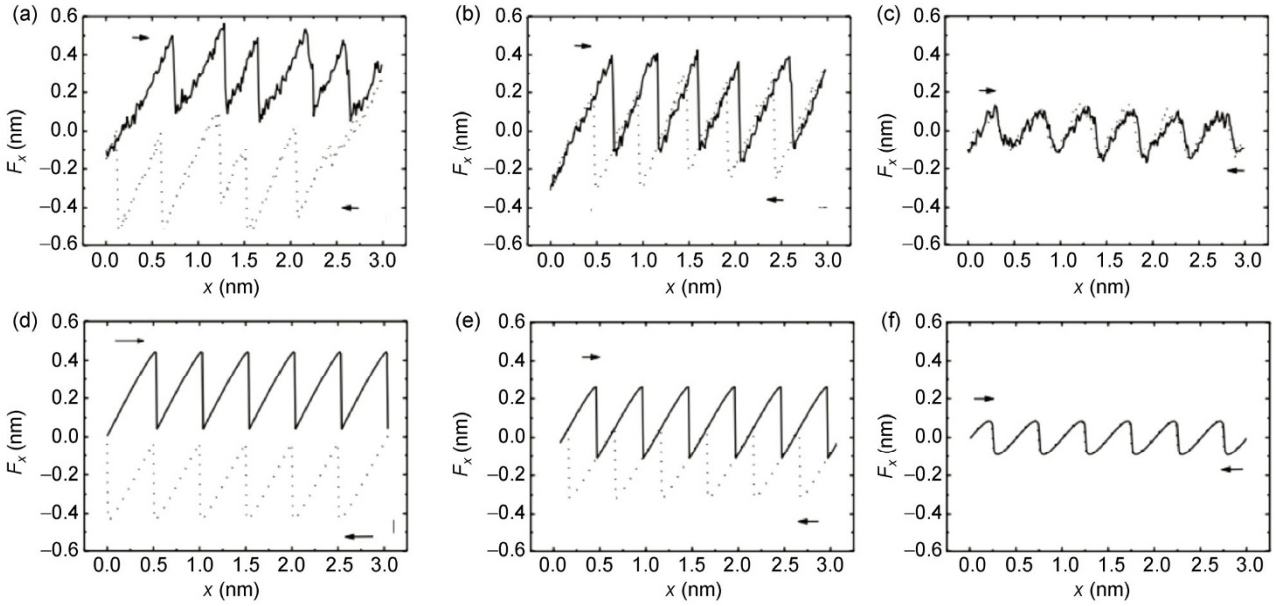

Fig. 4 (a)–(c) Measurements of the lateral force acting on the tip sliding forward and backward in (100) direction over a NaCl (001) surface. The externally applied load was (a) F_N = 4.7 nN, (b) F_N = 3.3 nN, and (c) F_N = 0.47 nN. (d)–(f) Corresponding numerical results from the PT model for (d) $\eta = 5$, (e) $\eta = 3$, and (f) $\eta = 1$. The stiffness was chosen as k = 1 N/m and the lattice constant as a = 0.5 nm. Note that for values of $\eta \leqslant 1$ the hysteresis loop enclosed between the forward and the backward scan vanishes, i.e., there is no more dissipation within this model [17].

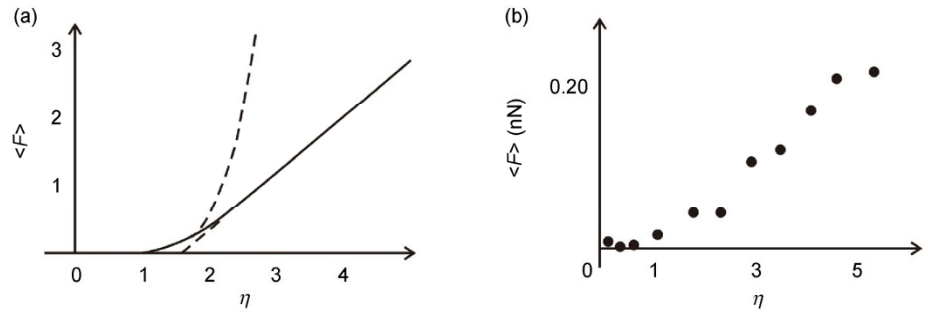

Fig. 5 (a) Analytical estimation of the mean lateral force <*F*> as a function of the parameter η in the one-dimensional PT model. The dashed curves correspond to the quadratic dependence and the linear dependence expected when $\eta \to 1$ and $\eta \to \infty$ respectively [18]. (b) Experimental dependence of <*F*>(η) as observed in the AFM measurements on NaCl (001) presented in Fig. 4. Each data point corresponds to an average over a two-dimensional scan of 3×3 nm^2 [17].

An alternative way to enter the regime of smooth sliding is to apply force modulations. In this case, the amplitude of the tip-surface interaction potential is modulated in time as $U_0(1+\alpha\sin(\omega t))$. Either mechanical or electrostatic force modulation can be used. In the latter case, the electrostatic force modulation is simply done by a bias voltage modulation, as in Fig. 6. Socoliuc et al. have observed that the application of a few volts across the piezoelement shaking the probing tip is sufficient to enter the dynamic superlubricity regime [19]. However, the applied frequency ω has to match the contact resonance frequency, which amplifies this effect strongly. It is found that the application of force modulations extends the regime of static lubricity and the analysis done in the "static" case can be retained introducing the parameter

$$\eta_{\text{eff}} = \frac{4\pi^2 U_0(1-\alpha)}{ka^2}.$$

In analogy to the static case, superlubricity is reached

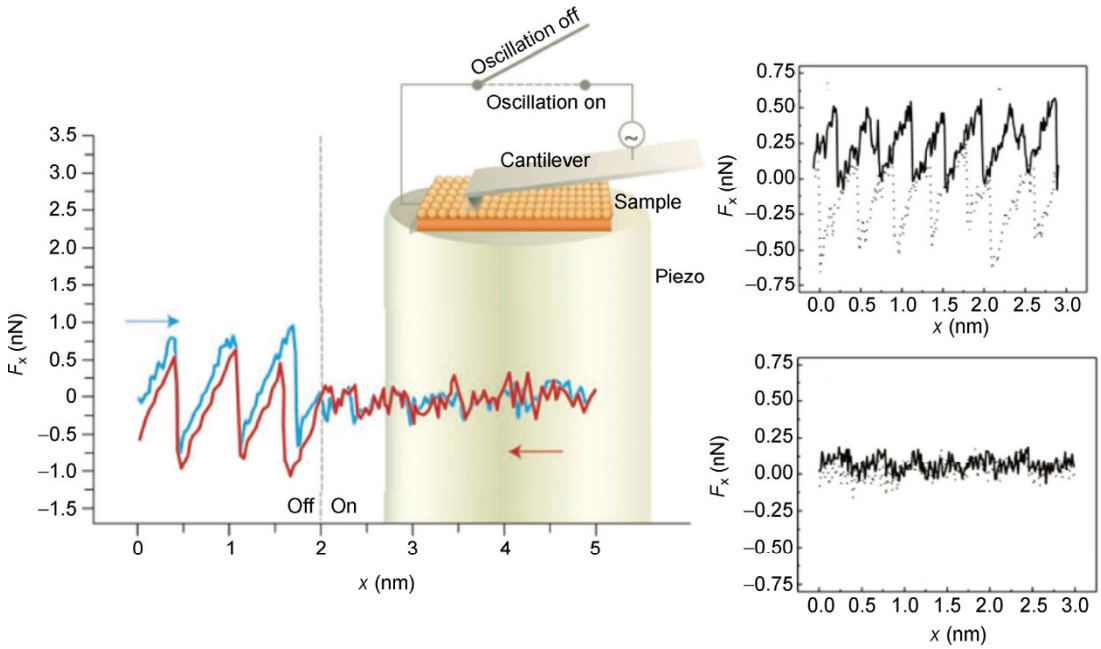

Fig. 6 The application of a force modulation at one of the contact resonance frequencies leads to a reduction of the average friction force <*F*>. The dynamic lubricity can help to extend the static lubricity to larger normal forces and to switch atomic friction on and off rapidly [24].

when η_{eff} is equal or smaller than 1. The stronger is the modulation the higher is the energy barrier which can be overcome. In this case, a map of the lateral force averaged over the oscillation cycles and acquired on a sample region precisely reproduces the tip-surface interaction potential in the same area, as seen in other AFM experiments on ionic crystals and graphite [20].

However, one has to take into account that the force modulation not only reduces the normal force but also increases the normal force during part of the cycle where the sinus function changes sign. This increase of normal force can become problematic leading to wear of the contact. Therefore, the range of α-values has to be chosen carefully. For appropriate values the reduction of friction can also be accompanied by a reduction of wear, as has been observed by Lantz et al. [21]. In this case, a sharp silicon tip was dragged over large distances of several hundreds of meters on a polymer surface. If a static normal force was applied, the probing tip became blunter, as confirmed by SEM images, and the resolution was deteriorating. If a force modulation was applied at one of the contact resonances, the tip wear was found to be negligible across those large distances.

A significant reduction of the average lateral force is also observed if a nanotip is shaken laterally instead of normally [22]. In this case, an accurate analytical relation between the shaking amplitude and the parameters of the PT model can be derived [23].

4 Thermolubricity

Thermal vibrations lead also to a reduction of friction on the nanoscale. This has been clearly demonstrated by a series of atomic stick-slip measurements on graphite performed by Jansen et al. using AFM [25].

In Fig. 7 we show the effect of thermal vibrations on stick-slip as expected from numeric simulations. According to the PT model, if the parameter $\eta \gg 1$ the maximum lateral force (which can be identified with the "static" friction in this case) at 0 K is given by Ref. [18]:

$$F_s = \frac{2\pi U_0}{a}$$

and the average lateral force is

$$\langle F \rangle \approx \frac{2\pi U_0}{a}\left(1-\frac{\pi}{\eta}\right) \quad (1)$$

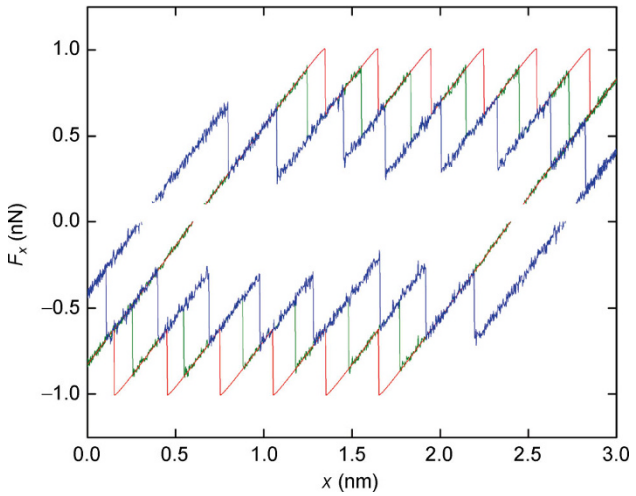

Fig. 7 Thermal excitation leads to reduction of friction. At 300 K (blue curves) the frictional forces are reduced to 75% compared to the values at 0 K. Their average values are 0.716 nN at 0 K (red curves), 0.586 nN at 100 K (green curves) and 0.429 nN at 300 K.

In Fig. 7 we have chosen the parameter values U_0 = 0.3 eV and a = 0.3 nm, which result in F_{max} = 1 nN (and η = 14). Introducing the Ermak-algorithm [26] to reproduce the effect of thermal vibrations, we observe a reduction of the frictional forces. The average force at 0 K is <F> = 0.716 nN, in agreement with Eq. (1), whereas at 100 K <F> = 0.586 nN and at 300 K <F> = 0.429 nN. Therefore, a reduction of friction of 75% is observed at 300 K compared to 0 K.

Explicit formulas to calculate the temperature and velocity dependence of the friction force can be derived [27, 28]. The most probable value of the peak force can be written as (for a derivation see Ref. [29]):

$$F_s(v,T) = F_s\left[1-\left(\frac{k_BT}{2\sqrt{2U_0}}\right)\left(\ln\frac{v}{v_0}\right)^{2/3}\right],$$

where

$$v_0 = \frac{\pi\sqrt{2}}{2}\frac{f_0 k_B T}{ka} \quad (2)$$

T is the temperature and k_B = 1.38 × 10^{-23} $m^2kg{\cdot}s^{-2}K^{-1}$ is the Boltzmann's constant. The parameter f_0 in Eq. (2) is the "attempt rate" of the thermally activated jumps. According to the Kramers' theory for thermally activated processes [30], if γ is the damping coefficient of the tip oscillations, the attempt rate is approximately given by $f_0 \approx \omega_0^2/(2\pi\gamma)$, where $\omega_0 \approx \sqrt{\eta k/m}$ and m is the effective mass of the sliding system (in the order of the cantilever mass).

The curves in Fig. 7 were determined assuming that k = 1.5 N/m, m = 10^{-12} kg and γ = 7.35 × 10^6 s^{-1}, i.e., slightly above the resonance (angular) frequency ω_0. Accordingly, we expect an attempt rate f_0 = 0.456 MHz, an average peak force of 0.57 nN, and an average force of 0.45 nN at v = 1 nm/s and T = 300 K, which is in good agreement with the results in the figure.

If the temperature is further increased or if the velocity is decreased, one enters the regime of thermolubricity, which was first described by Krylov et al. [31]. In this case, stick slip disappears and continuous sliding with minimum friction losses is observed. In this regime, friction becomes proportional to velocity, as it is the case for Brownian motion:

$$F_s(T,v) = \alpha(T)v = \frac{k}{2\pi f_0}\frac{2U_0}{k_BT}\exp\left(-\frac{2U_0}{k_BT}\right)v.$$

Krylov and Frenken [32] also argued that the oscillations in the contact zone should be treated separately introducing an additional spring with very high resonance frequency. This would lead to corrections of the friction force at low values of the parameter η. On the experimental side, the linear velocity regime has not yet been explored so far. However, thermolubricity most probably has an effect on the transition from stick slip, where the superlubricity regime might be enlarged.

Acknowledgements

E. M. acknowledges financial support by the Swiss National Science Foundation (SNF), the Commission for Technology and Innovation (CTI), COST Action MP1303 and the Swiss Nanoscience Institute (SNI). E. G. acknowledges the Spanish Ministry of Economy and Competitiveness (MINECO) Project MAT2012-26312.

References

[1] Braun O, Naumvets, A. Nanotribology: Microscopic mechanisms of friction Surf. *Sci Rep* **60**: 79–158 (2006)

[2] McGuiggan P M, Israelachvili J N. Adhesion and short-range force between surfaces. Part II: Effects of surface lattice mismatch. *J Mater Res* **5**: 2223–2231 (1990)

[3] Hirano M, Shinjo K, Kaneko R, Murata Y. Anisotropy of frictional forces in muscovite mica. *Phys Rev Lett* **67**: 2642–2645 (1991)

[4] Müser M H. Structural lubricity: Role of dimension and symmetry. *Europhys Lett* **66**: 97 (2004)

[5] Dienwiebel M, Verhoeven G S, Pradeep N, Frenken J W M, Heimberg J A, Zandbergen H W. Superlubricity of graphite. *Phys Rev Lett* **92**: 126101 (2004)

[6] Verhoeven G S, Dienwiebel M, Frenken J W M. Model calculations of superlubricity of graphite. *Phys Rev B* **70**: 165418 (2004)

[7] Filippov A, Dienwiebel M, Frenken J W M, Klafter J, Urbakh M. Torque and twist against superlubricity. *Phys Rev Lett* **100**: 046102 (2008)

[6] de Wijn A S, Fusco C, Fasolino A. Stability of superlubric sliding on graphite. *Phys Rev E* **81**: 046105 (2010)

[7] Zheng Q, Jiang B, Liu S, Weng Y, Lu L, Xue Q, Zhu J, Jiang Q, Wang S, Peng L. Self-retracting motion of graphite microflakes. *Phys Rev Lett* **100**: 067205 (2008)

[8] Liu Z, Yang J, Grey F, Liu J Z, Liu Y, Wang Y, Yang Y, Cheng Y, Zheng Q. Observation of microscale superlubricity in graphite. *Phys Rev Lett* **108**: 205503 (2012)

[9] Yang J R, Liu Z, Grey F, Xu Z P, Li X D, LiuY L, Urbakh M, Cheng Y, Zhen Q S. Observation of high-speed microscale superlubricity in graphite. *Phys Rev Lett* **110**: 255504 (2013)

[10] Martin J M, Donnet C, Le Mogne T, Epicier T. Superlubricity of molybdenum disulphide. *Phys Rev B* **48**: 10583–10586 (1993)

[11] Crossley A, Kisi E H, Bennet Summers J W, Myhra S. Ultra-low friction for a layered carbide-derived ceramic, Ti_3SiC_2, investigated by lateral force microscopy (LFM). *J Phys D: Appl Phys* **32**: 632–638 (1999)

[12] Yu M-F, Oleg Lourie O, Dyer M J, Moloni K, Kelly T F, Ruoff R S. Strength and breaking mechanism of multiwalled carbon nanotubes under tensile load. *Science* **287**: 637–640 (2000)

[13] Cumings J, Zettl A. Low-friction nanoscale linear bearing realized from multiwall carbon nanotubes. *Science* **289**: 602–604 (2000)

[14] Zheng Q S, Jiang Q. Multiwalled carbon nanotubes as gigahertz oscillators. *Phys Rev Lett* **88**: 045503 (2002)

[15] Jensen K, Mickelson C G W, Zettl A. Tunable nanoresonators constructed from telescoping nanotubes. *Phys Rev Lett* **96**: 215503 (2006)

[16] Kawai S, Koch M, Gnecco E, Sadeghi A, Pawlak R, Glatzel T, Schwarz J, Goedecker S, Hecht S, Baratoff A, Grill L, Meyer E. Quantifying the atomic-level mechanics of single long physisorbed molecular chains. In *Proceedings of the National Academy of Sciences of USA*, 2014: 3968–3972.

[17] Socoliuc A, Bennewitz R, Gnecco E, Meyer E. Transition from stick-slip to continuous sliding in atomic friction: Entering a new regime of ultralow friction. *Phys Rev Lett* **92**: 134301 (2004)

[18] Gnecco E, Roth R, Baratoff A. Analytical expressions for the kinetic friction in the Prandtl-Tomlinson model. *Phys Rev B* **86**: 035443 (2012)

[19] Socoliuc A, Gnecco E, Maier S, Pfeiffer O, Baratoff A, Bennewitz R, Meyer E. Atomic-scale control of friction by actuation of nanometer-sized contacts. *Science* **313**: 207–210 (2006)

[20] Gnecco E, Socoliuc A, Maier S, Gessler J, Glatzel, Baratoff A, Meyer E. Dynamic superlubricity on insulating and conductive surfaces in ultra-high vacuum and ambient environment. *Nanotechnology* **20**: 025501 (2009)

[21] Lantz M A, Wiesmann D, Gotsmann B. Dynamic superlubricity and the elimination of wear on the nanoscale. *Nat Nanotechnol* **4**: 586–591 (2009)

[22] Roth R, Fajardo O Y, Mazo J J, Meyer E, Gnecco E. Lateral vibration effects in atomic-scale friction. *Appl Phys Lett* **104**: 083103 (2014)

[23] Fajardo O Y, Gnecco E, Mazo J J. Out-of-plane and in-plane actuation effects on atomic-scale friction. *Phys Rev B* **89**: 075423 (2014)

[24] Carpick R. Controlling friction. *Science* **313**: 184–185 (2006)

[25] Jansen L, Hölscher H, Fuchs H, Schirmeisen A. Temperature dependence of atomic-scale stick-slip friction. *Phys Rev Lett* **104**: 256101 (2011)

[26] Allen M, Tildesley T. *Computer Simulations of Liquids*. Oxford (UK): Clarendon, 1990.

[27] Sang Y, Dube M, and Grant M. Thermal effects on atomic friction. *Phys Rev Lett* **87**: 174301 (2001)

[28] Riedo E, Gnecco E, Bennewitz R, Meyer E, Brune H. Interaction potential and hopping dynamics governing sliding

friction. *Phys Rev Lett* **91**: 084502 (2003)

[29] Gnecco E, Meyer E. *A Modern Approach to Friction.* Cambridge (UK): Cambridge University Press, in preparation.

[30] Kramers H A. Brownian motion in a field of force and the diffusion model of chemical reactions. *Physica* **7**: 284–304 (1940)

[31] Krylov S Y, Jinesh K B, Valk H, Dienwiebel M, Frenken J W M. Thermally induced suppression of friction at the atomic scale. *Phys Rev E* **71**: 065101(R) (2005)

[32] Krylov S Y, Frenken J W M. Thermal contact delocalization in atomic scale friction: A multitude of friction regimes. *New J Phys* **9**: 398 (2007)

Ernst MEYER. He received his PhD degree from the University of Basel, Switzerland, in 1991. He joined the faculty of the Department of Physics of the University of Basel in 1997. His current position is full professor of experimental physics and member of the Swiss Nanoscience Institute. His research interests are scanning probe microscopy, nanomechanics and nanotribology.